Performance Improvement of RADAR Imaging Using Machine Learning Techniques

Capstone Report

Yertas Zhumabekov

Nazarbayev University
Department of Electrical and Computer Engineering
School of Engineering and Digital Sciences

This project report was created on TexStudio editing platform using LaTeX. All the figures were drawn using draw.io online software tool.

NAZARBAYEV UNIVERSITY

Electrical and Computer Engineering
Nazarbayev University
http://www.nu.edu.kz

Title:
Performance Improvement of RADAR Imaging Using Machine Learning Techniques

Theme:
Theme

Project Period:
Spring 2024

Project Group:
IDSN-Lab

Participant(s):
Yertas Zhumabekov

Supervisor(s):
Carlo Molardi
Ikechi Ukaegbu

Copies: 1

Page Numbers: 17

Date of Completion:
April 26, 2024

Abstract:

The project aims to facilitate the progress of radar-based or complemented computer vision. The objective of the project is to perform a multi-purpose radar system that can complete object recognition and classification tasks. The machine learning techniques are used to carry out analysys of vast amount of data generated by the radar.

Contents

Preface

Radar imaging technology has evolved from its origins as a basic detection tool to a sophisticated system capable of high-resolution object observation and classification. Integration of machine learning can facilitate extending the capabilities and analysis of the radar systems improving object detection, classification, and recognition. The research in this direction holds significance because it can find applications across various domains, including environmental monitoring, defense, and autonomous systems. As technology continues to progress, radar imaging is poised to play an even more significant role in our ability to understand, classify, and respond to objects in our environment.

Nazarbayev University, April 26, 2024

Yertas Zhumabekov
<yertas.zhumabekov@nu.edu.kz>

Chapter 1

Introduction

Object detection, tracking, and identification are crucial in various fields such as autonomous vehicles, surveillance systems, and industrial automation. These technologies enhance safety, optimize resource utilization, and streamline operations in today's dynamic and interconnected world. Conventionally, object detection and tracking solutions had been relying on light-based sensors such as cameras and lidar [1]. However, the performance of such solutions was found to be rapidly deteriorating in challenging visual conditions (rain, dust, smoke, etc.) [2]. Given the shortcomings of these tools, radar systems accompanied by algorithms and machine learning techniques are becoming viable in various solutions [3] such as autonomous vehicles [4], robotics solutions [5], object tracking [6], simultaneous localization, and mapping [7].

The mmWave radar transmits a mmWave signal into space by striking an object, and this signal gets reflected. An intermediate-frequency (IF) signal is created by combining the echo signal, which is picked up by the receiving antenna, with a transmitting signal. Further post-processing and analysis of the IF signal helps to determine the existence, location, and attributes of the object. The object's distance can be determined by the time lag between signal transmission and reception, its motion speed and direction can be determined by the phase and Doppler effect, and its size and shape can be inferred from the amplitude reflected signal [8].

Due to its distinctive capabilities to identify the location, movement, and shape of the object, radar technology serves as an excellent surveillance tool. Within it, object detection and recognition are extensively studied areas leading to the development of methods of classification. Generally, the development of solutions for object detection and recognition puts emphasis on aspects such as methodologies of signal acquisition, signal processing, precision improvement, as well as optimal implementation of machine learning techniques [6]. In this regard, there are some works and findings useful for consideration.

One of the methods that are utilized for classification purposes in radar systems is through radar cross-section (RCS). In essence, RCS is a measure of power scattered by objects in a given direction when illuminated by radar [8]. There are RCS-based classification solutions: radar micro-Doppler analysis that considers motion and vibration patterns of moving objects [9], and statistical recognition systems by measuring horizontal and vertical polarization RCS [10].

Several works proposed ways of target localization as well as classification using range-angle images [11] [12], rotating Frequency Modulated Continuous Wave (FMCW) radar [13], as well as synthetic aperture radar techniques [14] [15]. With the fixed position of the radar getting information of distance and reflected power is possible. On the other hand, properties of the shape can be inferred by introducing some change in the angle or position of each consecutive data takes. For example, by aligning radar along the elevation angle and gathering data in conjunction with rotating radar, it is possible to identify information such as height and width from radar signal imaging [11]. Similarly, by the synthetic aperture radar (SAR) method, which is effectively capturing data at different points along the azimuth line 2D radar imaging is possible [16] [17]. However, this method has its limitations as the radar system has no way of knowing from which elevation angle reflection is coming from. This along with the big beamwidth of the radar creates issues with elevation ambiguity and cannot be fully addressed by only using radar systems, but requires cooperation and fusion with lidar or camera [18].

From the results of the other works it becomes evident that the data captured with radar systems generates huge amounts of information that only can be sensible through the implementation of machine learning techniques. Machine learning algorithms such as Logistic Regression, Naive Bayes [19] as well as Newral Networks [20] [21] [22] are possible implementations for data analysis and classification.

This work aims to work out an object classification solution by relying on the information from a 1D Range-FFT plot as well as utilizing a SAR-like methodology of radar shifting. The investigation aims to differentiate among various object types as well as to identify changes in characteristics within the same type of object.

Chapter 2

Methodology

2.1 Setting up and working with radar

To begin the work the radar system should be properly set up. First, the correct interface between radar and data collecting DCA 1000 board should be achieved by a toggled set of switches and pins. The Matlab Runtime Engine should be downloaded along with a few specific drivers. Also, there should be a connection between the radar and the evaluation program running the computer through the USB and Ethernet cables. Finally, the mmWave Studio software is downloaded where all possible configurations of the radars can be set. Through the software, the properties of the transmitted signal such as starting frequency, sampling frequency, bandwidth, sampling duration, number of samples, and many others can be manipulated according to the requirements of the experiment. The mmWaveStudio provides some plots by performing several methods of signal processing. Nevertheless, all of the signal processing processes should be replicated since the program doesn't allow to recording of any data from its analysis.

Therefore raw data extraction and preparation for further work is a crucial step in working with IWR1843 radar. The DCA1000 performs data collection and captures information over four LVDS lanes where each corresponds to a specific receiver. The data samples are represented as two-byte elements and follow the two's complement format, thus the recorded data is in the '.bin' extension. The received data structure can be observed in Fig. 2.1 where each reading from every receiver is stored in a separate row. In the case of a complex data format, the first set of rows comprises real data, while the subsequent rows contain imaginary data. Leveraging the properties outlined in the data collection manual, a meticulous process is employed to convert the raw data into a ready-to-work format, facilitating seamless integration into the signal processing workflow.

2.2 Experimental setup

With the hardware and software components in place and by being able to post processing data it is safe to proceed to conducting radar experiments. By using the aforementioned radar system configuration it is possible to do experiments that involve target tracking, distance measurement, or velocity estimation. This work employs the experimental procedure as depicted in Fig 2.2. In this procedure, N number of measurements are taken with changing radar position and constant object location. The radar is shifted with constant step distance along the horizontal line. The distance between the object and radar, the overall length of radar shifting, as well as step size, can be configured by the experiment conducter. For each step, the sampled data by DCA1000 is recorded and saved.

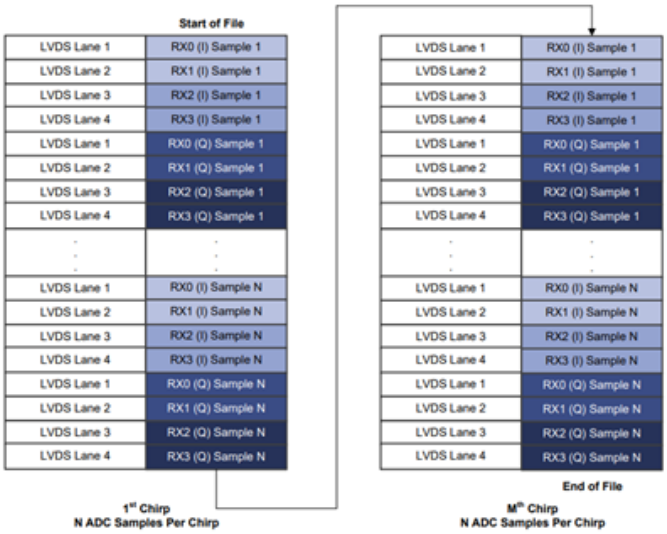

Figure 2.1: Visualization of the recorded data by DCA 1000.

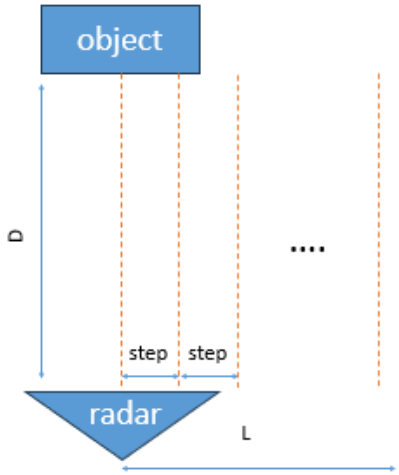

Figure 2.2: Experimental setup for the classification task.

Chapter 3

Results and Discussions

The main purpose of the project is the query of the betterment of radar technology. Thus, an extensive understanding of the radar system is required. For that purpose, practical experience of working with radar as well as any desired working setup and data is acquired by the IWR1843 radar. The collected data is then processed using the mmWaveStudio software. The vast functionality of the radar allowed to us collect data using a variety of settings and objects. The DCA1000 is an additional plate in the radar system that is responsible for storing the readings. The uniqueness of this system is that only the beat signal between the radar's transmitter and the received signal is saved. Fig 3.1 demonstrates the internal structure of radar showcasing that sampling happens after multiplying the input and output signals.

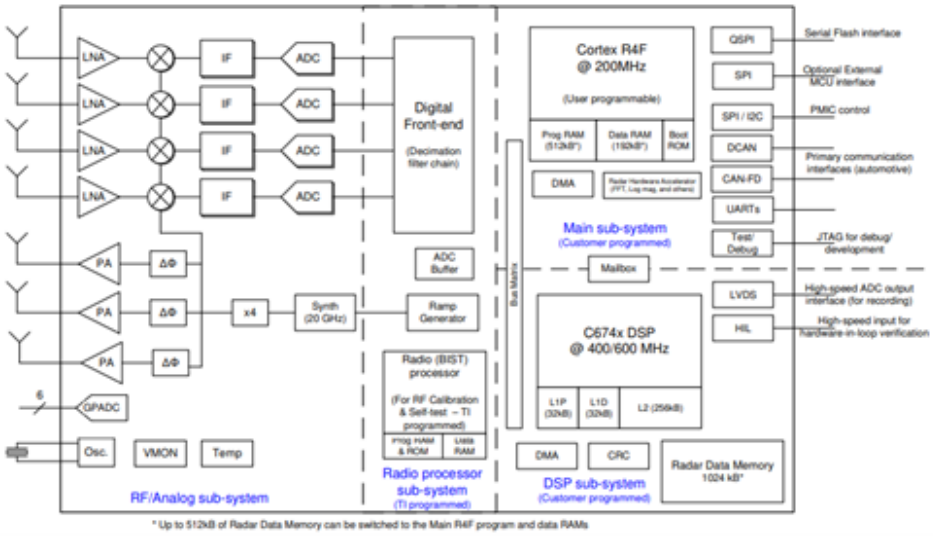

Figure 3.1: Internal structure of the IWR1843 radar

3.1 Basic signal processing

The signal processing techniques were applied to the stored data for extraction of the desired information such as the number of the object(s), location, and reflected power. The basic analysis of the signal in this project is to define the object(s) in range, time vs. amplitude, and time vs. frequency. As it was discussed in the previous part, due to the data collection approach of DCA 1000 there is a necessity for some reconfiguration of the collected data. Steps such as collecting correct rows of data in other words from the working receiver, and converting 2's complement binary data to signed decimal data were performed to get the sampled intermediate frequency signal.

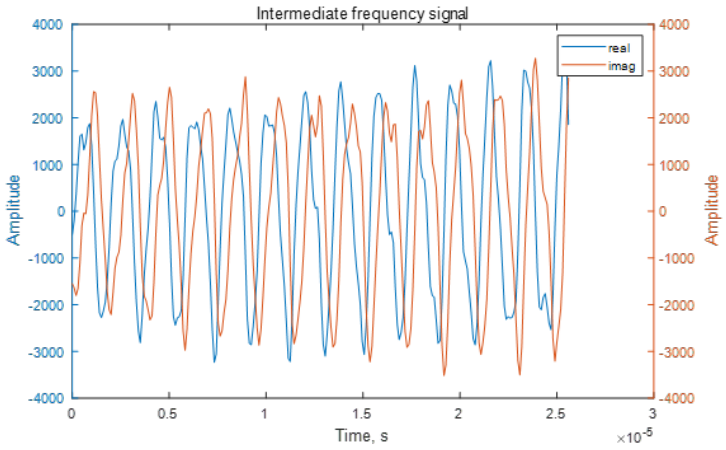

Figure 3.2: ADC sampled beat signal.

The beat signal plays a vital role in object detection and range location in the Linear Frequency Modulated (LFM) radar system. The radar itself emits a continuous sinusoidal signal with increasing frequency over time. At some point, this signal gets reflected from the object and returns to the radar. As it was noted before in radar circuitry transmitted and received signals are multiplied to form beat frequency. In other words, each object depending on its distance from the radar generates a specific beat frequency. As a result, the Fourier analysis of the beat signal should present the locations of objects. Additionally, by using the following formula location of the object corresponding to a specific beat frequency can be identified as:

$$R_n = \frac{c * f_{bn}}{2\alpha}$$

Where R_n is range of n's object, c is light speed, f_{bn} is beat frequency, and α is slope of chirp.The range values can be calculated using user-defined information such as sampling rate and number of samples used. Since the data should pass through ADC sampling the maximum beat frequency is the sampling rate. By using this information, the maximum range value can be identified for the highest beat frequency. The number of samples defined by the user can help in identifying discrete range values. The Fourier transform of the beat signal and change of scale to logarithmic results in the range vs. Power of the signal which demonstrates reflected power throughout the whole possible range values. The object present in the scene is depicted as a peak in this plot. By taking the differentiating of the Range vs. Power plot and tracking the change of derivative sign from positive to negative it is possible to pinpoint the location of the peaks in the Power vs. Range plot. This information is essential because after sorting derivative peaks by the values of the reflected power it is possible to obtain and save the true locations of the objects in the scene.

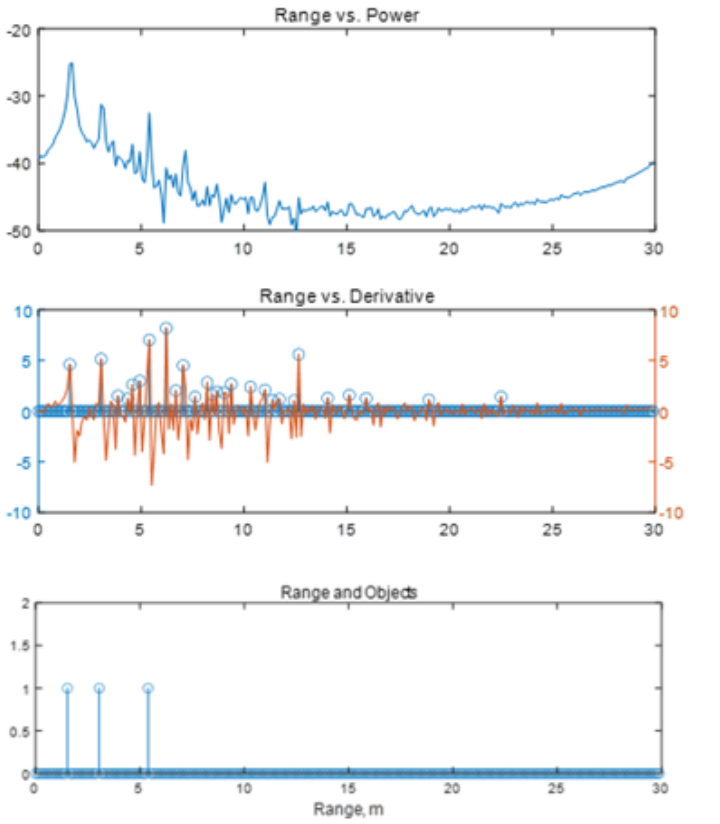

Figure 3.3: Results of the signal processing.

The signal of the LFM radar can also be described by the chirp frequency profile. The desired signal features such as signal duration, slope, number of samples, ADC start time and many other features can be chosen. Fig 3.4 which is the chirp profile demonstrates the time and frequency relation of the transmitted signal. The signal duration was 100 µs with a slope of the 39.9 MHz/µs which corresponds to the maximum bandwidth of 4GHz of the radar. However, only some part of the signal is sampled and stored. Since the sampling time is 10MHz, the sampling duration is governed by the configured number of samples. During the work the default number of sampels which is 128 samples were used that correspond to the 128 µs. The chirp signals with this configuration were sent from the transmitter and were reflected back. As a result, the reflected signal could be depicted as the time-delayed version of the transmitted signal. From this figure, it is possible to track round trip delay and identify/confirm the range information of the object.

The following sinusoidal function can represent the LFM signal's real part.

$$x(t) = sin(2\pi * \frac{\alpha}{2} * t^2)$$

The transmitted signal is defined through a simple FM-modulated sinusoidal signal and can be shown in Figure 3.6. As its bandwidth is in terms of GHz the zoomed-in version is shown for more distint visualization. The radar system does not record the received signal but it can be replicated by delayed versions of the transmitted signal. Lastly, summation of reflected signals together yields in the overall signal seen by the receiver as in Fig 3.7.

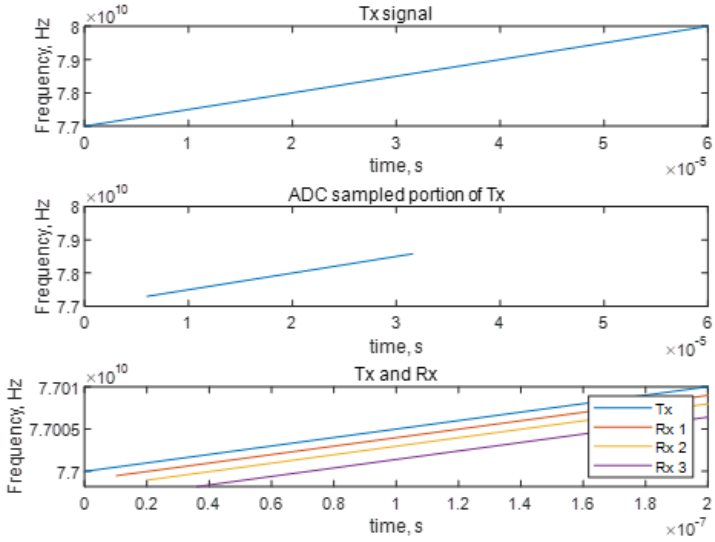

Figure 3.4: Chirp profile of Tx and Rx.

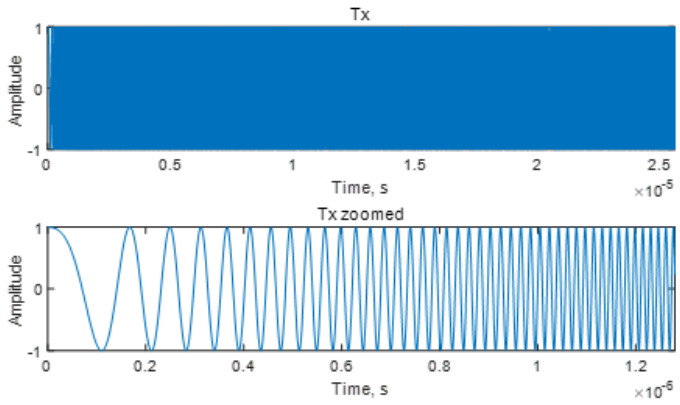

Figure 3.5: Transmitted chirp signal.

The degree of similarity of the transmitted and received signal can be tested using cross-correlation. The cross-correlation signal processing tool points out exactly at which points the two signals resemble each other the most. Since the received signal is the summation of several time-delayed chirp signals, the correlation outcome would be described by a number of objects and time delays. The significance of the cross-correlation analysis is that it can encompass a few results such as the number of detected objects as well as values of time delays with which the signal is received [23].

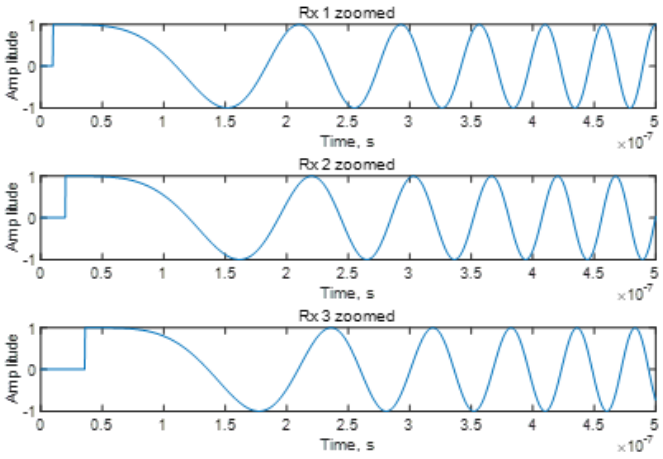

Figure 3.6: Time delayed chirp signals reflected from each object

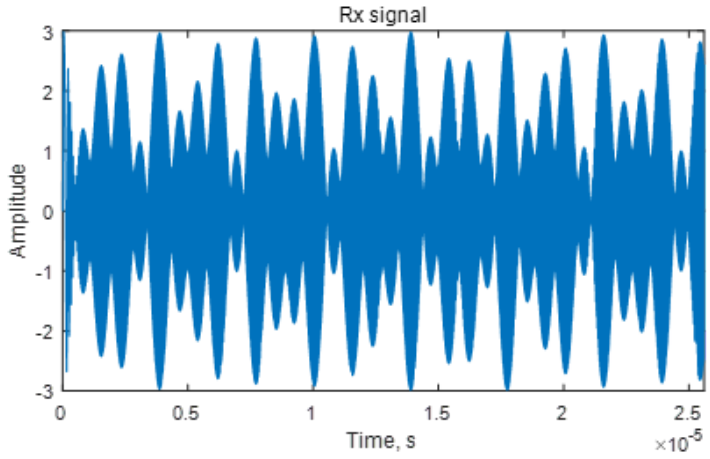

Figure 3.7: Combined chirp signals at receiver

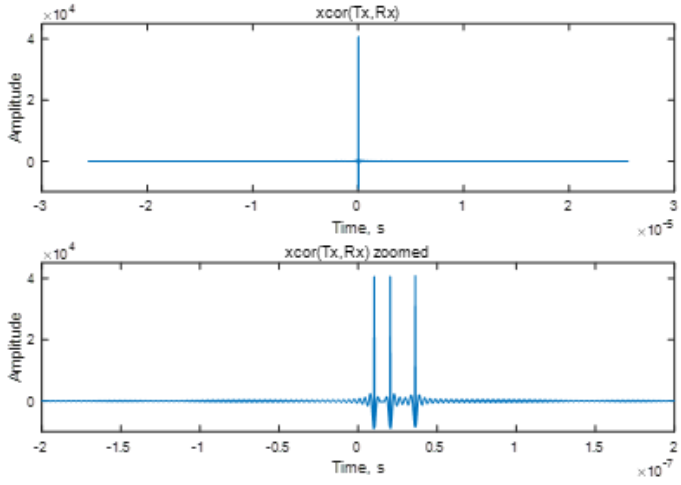

Figure 3.8: Cross correlation of transmitted and received signal.

3.2 Object classification

There were efforts on performing an object classification algorithm relying on the obtained distance against FFT values using the radar range equation and RCS values [10].

$$S_{db} = P_{T_{db}} + 2G_{db} + 10log_{10}(\frac{\lambda^2}{(4\pi)^2}) - 40log_{10}R - L_{db}$$

Where S_{db} is received power of the radar, $P_{T_{dB}}$ is transmitted power, G_{db} is gain of tranmitter and receiver, R is range or distance of the object from radar, and L_{db} is system losses

The radar components identified in the data extraction part as well as range and respective power components contribute to most of the variables in an equation. The only unknowns are RCS and the Losses of the system. The Radar Handbook text describes various types of losses that can occur in a radar system. These include transmit losses, receive losses, atmospheric losses, scanning or beam shape losses, range-gate straddling losses, Doppler straddling losses, collapsing losses, signal processing losses, and miscellaneous losses [24]. The values for these losses depend on factors such as radar operating frequency, range to target, elevation angle, and specific radar system design. Since these parameters and environment can be held constant it was hypothesized that an equal amount of range from the object their loss value will be similar. Additionally, many researcher results agree that RCS value is dependent on the radar surfacing shape rather than area [24]. Nevertheless, due to insufficient information about the losses in the radar system and its components, as well as the challenge of precisely measuring power losses attributable to various shapes, no effective solution for classification using the range equation, power, and losses have been developed. Also, it was found that relying on a single recorded data point as the basis for classification poses a significant limitation due to its inability to account for the inherent diversity among objects. This approach fails to capture the nuanced variations in shape and characteristics, rendering it impractical for accurate classification. The single shot detection method employed so far overlooks the object's distinctive features, leading to a lack of possible distinction between different objects.

It was found that the Radar Cross Section (RCS) of an object undergoes dynamic changes as the position and angle of either the radar or the object is altered [10]. The RCS, representing the object's reflectivity, is intricately linked to the incident angle of radar waves. A shift in the position could introduce variations in the amount of the received power of the radar. It is thought that different levels of the reflected powers can be achieved by changing the radar recording position and the reflected signal's trajectory change. In other words, this method observed the unique power level patterns that are formed after signal scattering of an object of interest at different radar positions. By systematically shifting the radar's lateral position and examining the corresponding reflected powers at varying locations along a single axis, a rudimentary yet effective method for object classification can be established.

This approach relies on discerning patterns in the reflected power as the radar lateral movement. The derived hypothesis is rooted in the behavior of radar waves interacting with different object geometries. Objects with low curvature are expected to exhibit a drastic power drop after a certain point where the radar waves cease to be effectively reflected. In contrast, objects with higher curvature or moderate radii are anticipated to maintain a relatively consistent reflected power, as the scattering of waves remains consistent despite variations in the angle of arrival. Additionally, the intensity of the power levels can reveal the surface area of an object and enable differentiation of objects within a single class based on changes in specific features. This lateral analysis of reflected power provides a simple, yet effective means of classifying simple objects based on their geometric characteristics.

By following the methodology steps as well as the experimental setup as in Fig 2.2 numerous experiments with different objects were completed. With each object, the 21 measurements with the stationary object are done with a 1.5 cm radar step. The power of the object was located and recorded on the table for the different shift positions. The measurements' outcomes were meticulously considered by standardizing the experiments by conducting experiments at the same place, as well as standardizing the surface material that reflects the radar signal from.

Fig 3.9 a, Fig 3.9 b, and Fig 3.10 a represent the change in the powers of the objects with different shapes such as cylindrical, spherical, and flat objects. The plots of cylindrical and spherical objects demonstrate the possibility of classification within the same class since the power levels of objects with different features are distinctive. In other words, objects with bigger radii hence with greater surface area reflect more power throughout the whole range than their counterparts with smaller radii. Other than that Figure 3.10 b showcases different trends of the power levels for different types of objects. Despite all of them having a comparable radius and length of 5 to 6cm, both the power change pattern as well as average power values vary significantly. Collected data, distinctions in the power levels and shape along with the changes in the slope from each successive shift were used in making a multiclass classifier model. Some of the analytical measurements confirming numerical differences in results are recorded in Tables 1 to 3.

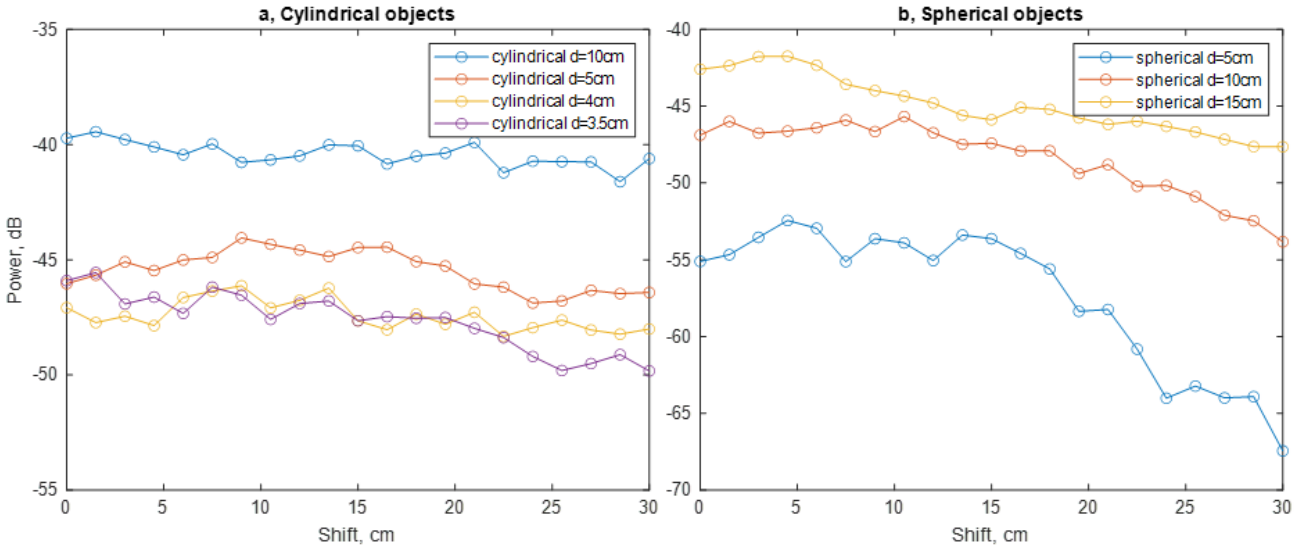

Figure 3.9: Power levels for the a) cylindrical b) spherical objects throughout shifts

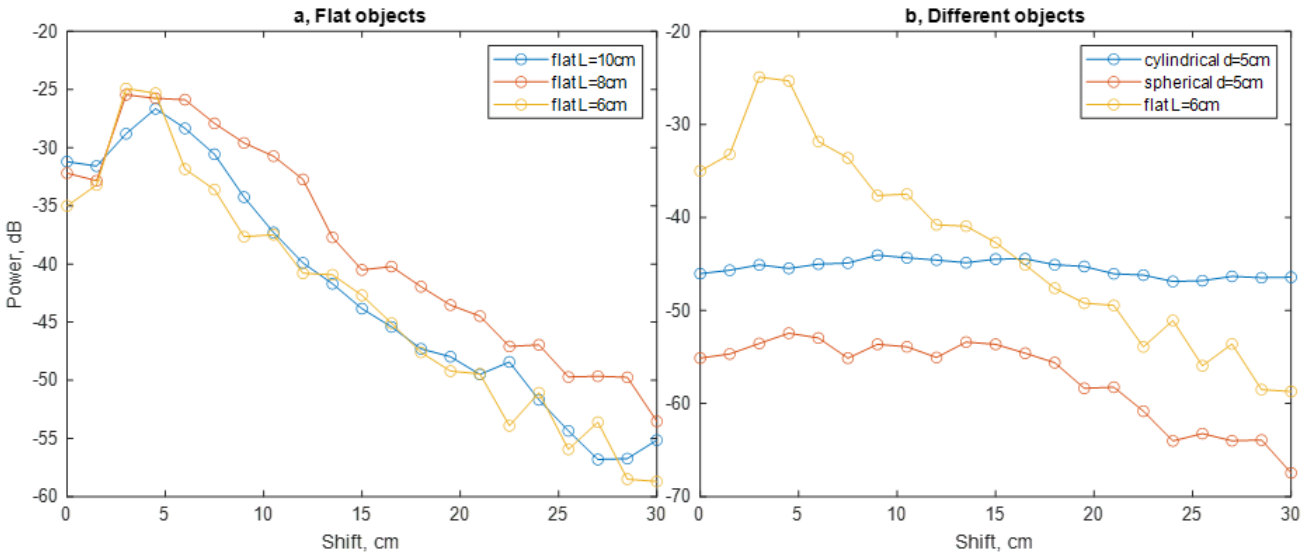

Figure 3.10: Power levels for the a) flat and b) different objects throughout shifts

Table 3.1: Analytical measurements from cylindrical objects' data

Type: Cylindrical	Diameter = 10	Diameter = 5	Diameter = 4
Average power	-39.50	-44.24	-46.14
Average slope	-0.978	-0.991	-0.977

Table 3.2: Analytical measurements from spherical objects' data

Type: Spherical	Diameter = 15	Diameter = 10	Diameter = 5
Average power	-43.73	-46.98	-55.39
Average slope	-0.879	-0.834	-0.706

Table 3.3: Analytical measurements from flat objects' data

Type: Flat	Length = 10	Length = 8	Length = 6
Average power	-41.23	-41.19	-37.40
Average slope	-0.430	-0.435	-0.491

3.3 Machine Learning

The overall processes involved in the development of the classifiers using the captured data aimed to evaluate and compare the results of various machine learning models. It involved some structured steps toward the performance evaluation and comparison of different machine learning models on other data characteristics. These stages include data preparation, model training, evaluation, cross-validation, and visualization. Data was first collected and formatted for all three kinds of objects: cylindrical, spherical, and flat. Each set of data readings was collected concerning the dimensions and changing features of the object (diameter, length, etc.) and labeled with the size category of the object, which would be the target label for classification. So, we arrange data in an array for each of the object types and then give shape to the data according to the requirement for sci-kit-learn, the machine-learning library used in the process.

Three different classifiers were trained on this data: k-nearest neighbors (kNN), Support Vector Machines (SVM), and Random Forest. Each one was trained on the proper training datasets and later tested using a simple train-test split to be checked for its performance. Such a composition of classifier models was selected with the intention of obtaining diverse classifying tools. For each model, the best-performing parameters were chosen using the GridSearch method. Also, ross-validation was used to prevent model overfitting to specific parts of the data as well as to confirm the output results with different sets of training data.

The comparison of the accuracy of three models and across object types was shown through bar charts in Fig 3.11, hence clearly indicating which classifier was outperforming others within each dataset. These visualizations were vital to making the findings clear and gave the reader both much detail and a high-level view of the classifier performances. The resulting graph, on which it is apparent how each classifier (k-Nearest Neighbors (kNN), Support Vector Machines (SVM), and Random Forest)) applied to three types of object measurements (cylindrical, spherical, and flat)) relates, gives essential insight into the way each model deals with the classification of physical measurements.

In the classification of the cylindrical object, kNN and SVM behaved at the same level, almost with the same accuracy: approximately 70.59'%'. Random forest was also okay but slightly worse, somewhere at about 64.71'%'. This could indicate that the cylindrical measurements are homogeneous or distributed so that the particular model is classified relatively easily. Spherical had the highest accuracy, followed closely by SVM and Random Forest, respectively, which tied for the highest at approximately 84.62'%'. The kNN also did quite well at 76.92'%'. The overall performance strength of all models with spherical measurements indicates that spherical measurements are distinct from and span separate features in space, allowing high-accuracy linear models like SVM.

For the class of flat objects, this was the worst class, whereby k-NN and SVM suffered drastically and could only fetch an accuracy level of approximately 23.08'%'. However, Random Forest emerged powerful, showing a much higher accuracy of 46.15'%' compared to other methods, indicating well how it would be able to deal with the likely complex distributions of flat object measurements, which possibly would be even overlapping, in contrast to linear or more straightforward models. Those results may be illustrations of the strengths and limitations of different models. The latter may constitute practical work for further classification methodology. Knn offers consistency in scenarios where class boundaries are clear but gives way in scenarios with unclear class boundaries or where additional data is heterogeneous.

SVM works best in high-dimensional spaces or could also work effectively in cases with a clear separation margin. Its performance on flat objects could signal limited use in more complex or intersected data distributions. Random forest shows robustness over all the datasets, but peculiarly, it does very well where most other models struggle. As an ensemble, this approach aggregates predictions from multiple decision trees, thus giving it the ability to better handle the complexity and variability.

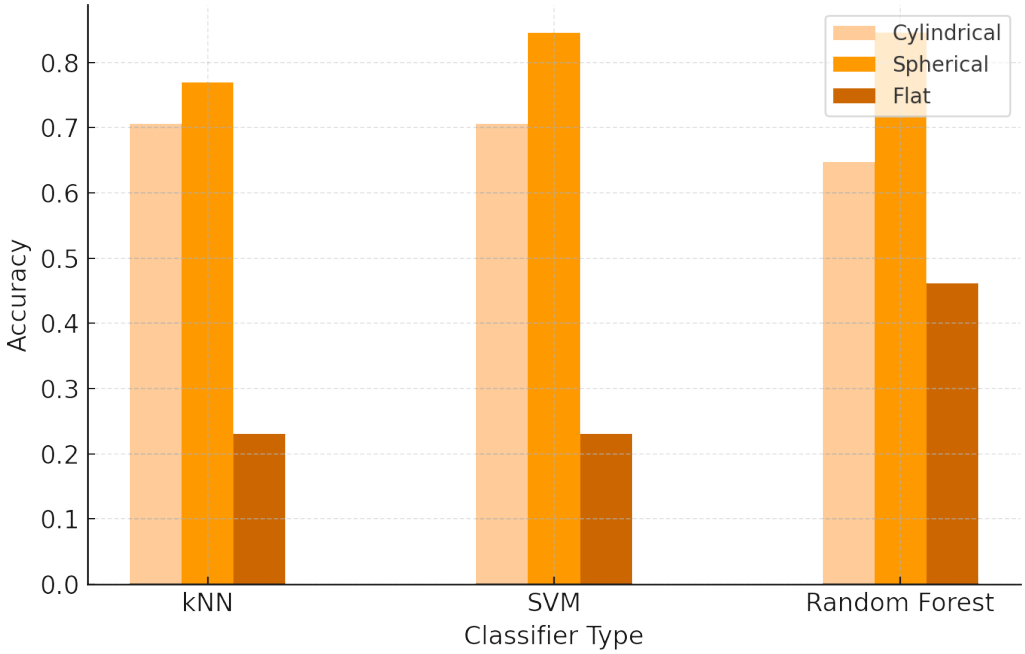

Figure 3.11: Classifier accuracies by object type

Chapter 4

Conclusion

In conclusion, the utilization of radar imaging has proven to be immensely valuable, allowing for the extraction of valuable information from the stored signals. The analysis of range vs. power plots, coupled with relevant hypotheses, not only enhances our understanding of the data but also holds the potential to pave the way for object classification. This integration of technology and theoretical frameworks opens new avenues for discerning meaningful insights from radar signals, marking a significant stride in the field. The methodologies employed in this work, such as signal processing, experimentation, and machine learning, have effectively demonstrated the potential of radar technology for classifying objects of different shapes. By analyzing the characteristics and power levels of reflected signals, distinct patterns corresponding to various object shapes were identified, and a machine learning classifier was developed to interpret these signals. The project showcases the feasibility of distinguishing between objects like flat, cylindrical, and spherical shapes with varying degrees of accuracy, setting the stage for further enhancements and broader applications in this promising field.

Bibliography

[1] Jakob Engel, Vladlen Koltun, and Daniel Cremers. "Direct Sparse Odometry". In: *IEEE Transactions on Pattern Analysis and Machine Intelligence* 40.3 (2018), pp. 611–625. DOI: 10.1109/TPAMI.2017.2658577.

[2] Yuen Peng Loh and Chee Seng Chan. "Getting to know low-light images with the Exclusively Dark dataset". In: *Computer Vision and Image Understanding* 178 (2019), pp. 30–42. ISSN: 1077-3142. DOI: https://doi.org/10.1016/j.cviu.2018.10.010. URL: https://www.sciencedirect.com/science/article/pii/S1077314218304296.

[3] A Soumya, C Krishna Mohan, and Linga Reddy Cenkeramaddi. "Recent Advances in mmWave-Radar-Based Sensing, Its Applications, and Machine Learning Techniques: A Review". In: *Sensors* 23.21 (2023), p. 8901.

[4] Arthur Venon et al. "Millimeter wave FMCW radars for perception, recognition and localization in automotive applications: A survey". In: *IEEE Transactions on Intelligent Vehicles* 7.3 (2022), pp. 533–555.

[5] Kyle Harlow et al. "A New Wave in Robotics: Survey on Recent mmWave Radar Applications in Robotics". In: *arXiv preprint arXiv:2305.01135* (2023).

[6] Andre Pearce et al. "Multi-Object Tracking with mmWave Radar: A Review". In: *Electronics* 12.2 (2023), p. 308.

[7] Martin Adams, Ebi Jose, and Ba-Ngu Vo. 2012.

[8] Bu-Chin Wang. *Digital signal processing techniques and applications in radar image processing*. John Wiley & Sons, 2008.

[9] Samiur Rahman and Duncan A Robertson. "Classification of drones and birds using convolutional neural networks applied to radar micro-Doppler spectrogram images". In: *IET radar, sonar & navigation* 14.5 (2020), pp. 653–661.

[10] Martins Ezuma et al. "Radar Cross Section Based Statistical Recognition of UAVs at Microwave Frequencies". In: *IEEE Transactions on Aerospace and Electronic Systems* 58.1 (2022), pp. 27–46. DOI: 10.1109/TAES.2021.3096875.

[11] Siddharth Gupta et al. "Target classification by mmWave FMCW radars using machine learning on range-angle images". In: *IEEE Sensors Journal* 21.18 (2021), pp. 19993–20001.

[12] Gianluca Ciattaglia et al. "Assessment of Displacement Measurements by a mmWave Radar". In: (2023), pp. 1–6. DOI: 10.1109/SAS58821.2023.10254086.

[13] Damien Vivet, Paul Checchin, and Roland Chapuis. "Localization and mapping using only a rotating FMCW radar sensor". In: *Sensors* 13.4 (2013), pp. 4527–4552.

[14] Uwe Aulenbacher et al. "Millimeter wave radar system on a rotating platform for combined search and track functionality with SAR imaging". In: 9252 (2014), p. 925202.

[15] Helena Cruz et al. “A Review of Synthetic-Aperture Radar Image Formation Algorithms and Implementations: A Computational Perspective”. In: *Remote Sensing* 14.5 (2022), p. 1258.

[16] Gang Xu et al. “High-Resolution mmWave SAR Imagery for Automotive Parking Assistance”. In: *IEEE Journal on Miniaturization for Air and Space Systems* 4.1 (2023), pp. 54–61. DOI: 10.1109/JMASS.2022.3226771.

[17] Hiroyoshi Yamada et al. “High-resolution 2D SAR imaging by the millimeter-wave automobile radar”. In: (2017), pp. 149–150. DOI: 10.1109/CAMA.2017.8273384.

[18] Akash Deep Singh et al. “Depth Estimation from Camera Image and mmWave Radar Point Cloud”. In: (2023), pp. 9275–9285. DOI: 10.1109/CVPR52729.2023.00895.

[19] Jyoti Bhatia et al. “Object Classification Technique for mmWave FMCW Radars using Range-FFT Features”. In: (2021), pp. 111–115. DOI: 10.1109/COMSNETS51098.2021.9352894.

[20] Jyoti Bhatia et al. “Object Classification Technique for mmWave FMCW Radars using Range-FFT Features”. In: (2021), pp. 111–115. DOI: 10.1109/COMSNETS51098.2021.9352894.

[21] Qiao Cheng et al. “Compressive sensing radar imaging with convolutional neural networks”. In: *IEEE Access* 8 (2020), pp. 212917–212926.

[22] Jingkun Gao et al. “Enhanced radar imaging using a complex-valued convolutional neural network”. In: *IEEE Geoscience and Remote Sensing Letters* 16.1 (2018), pp. 35–39.

[23] Fangming Liu et al. “Isar imaging and cross-range scaling based on image rotation correlation”. In: *Journal of Beijing Institute of Technology* 31.2 (2022), pp. 196–207.

[24] Mohinder Jankiraman. *FMCW radar design*. Artech House, 2018.

[25] Vladimir Díaz Charris and José Manuel Gómez Torres. “Analysis of radar cross section assessment methods and parameters affecting it for surface ships”. In: *Ciencia y tecnología de buques* 6.11 (2012), pp. 91–106.